Diffusivity of native defects in GaN

Sukit Limpijumnong[1,2] and Chris G. Van de Walle[1]
[1]*Palo Alto Research Center, 3333 Coyote Hill Road, Palo Alto, California 94304, USA*
[2]*School of Physics, Institute of Science, Suranaree University of Technology, Nakhon Ratchasima, Thailand*
(Received 26 September 2003; published 27 January 2004)

The diffusion of relevant native point defects in wurtzite GaN crystals is investigated using first-principles density-functional pseudopotential calculations. Our reexamination of the ground state of the defects, using a higher level of convergence than was previously used, yields results in good agreement with earlier published results [J. Neugebauer and C. G. Van de Walle, Phys. Rev. B **50**, 8067 (1994)]. Gallium interstitials are stable at the octahedral interstitial site and can occur in 1+, 2+ (metastable), or 3+ charge states. They migrate via an interstitialcy mechanism with an unexpectedly low barrier of 0.9 eV, consistent with the annealing of the $L5$ signal in electron-paramagnetic-resonance experiments [K. H. Chow *et al.*, Phys. Rev. Lett. **85**, 2761 (2000)]. For the nitrogen interstitial the ground-state configuration is a split interstitial, occurring in charge states ranging from 1− to 3+. Migration also proceeds via an interstitialcy mechanism, with barriers of 2.4 eV or lower, depending on the charge state. The nitrogen vacancy has two stable charge states 1+ and 3+. The migration barrier for V_N^+ is high (4.3 eV), while the migration barrier for V_N^{3+} is significantly lower, at 2.6 eV, consistent with recent positron-annihilation experiments [S. Hautakangas *et al.*, Phys. Rev. Lett. **90**, 137402 (2003)]. The gallium vacancy, finally, can occur in charge states 0, 1−, 2−, and 3−, and migrates with a barrier of 1.9 eV. For all these defects the lowest-energy migration path results in motion both parallel and perpendicular to the c axis; no anisotropy in the diffusion will therefore be observed. Applications to point-defect-assisted impurity diffusion will also be discussed.

DOI: 10.1103/PhysRevB.69.035207 PACS number(s): 61.72.Bb, 66.30.Hs, 71.55.Eq, 61.72.Ji

I. INTRODUCTION

Knowledge of the diffusion properties of native point defects is important to assess the likelihood of their incorporation during growth and processing; in addition, it forms the basis for understanding impurity diffusion, which is nearly always mediated by native defects. Diffusion also plays an important role in device degradation. Information about diffusion in nitrides is currently limited. Only a few experimental studies have been performed, and in some cases the results may reflect phenomena induced by the presence of a large concentration of extended defects, causing the results to be of limited applicability to bulk GaN.

To date, direct experimental studies of point-defect motion have been performed with three techniques: self-diffusion in isotope structures, electron paramagnetic resonance (EPR), and positron annihilation. Monitoring the diffusion of isotopes is a very direct and powerful way of studying diffusion. Only one such study has been carried out so far; by Ambacher *et al.*[1] EPR studies were performed by the group of Watkins[2–5] on point defects created by electron irradiation at low temperature. The one defect that has been unambiguously identified in these studies is the gallium interstitial (Ga_i), which was found to become mobile at temperatures slightly below room temperature. Our calculations will show that the migration barrier for Ga_i is indeed very low (0.9 eV), due to an interstitialcy migration mechanism.[6] The positron-annihilation studies, by the group of Saarinen,[7–9] are sensitive to vacancy defects, and have produced estimates for the migration barriers of gallium[8] and nitrogen[9] vacancies. None of these studies have systematically tracked diffusion over a range of temperatures; estimates of migration barriers are based mainly on observations of the temperatures at which the defects become mobile. In addition to the point-defect studies, some results have been reported on impurity diffusion.[10–13] Only diffusion coefficients at a given temperature were reported.

We have performed a comprehensive computational study tracking the diffusion paths of various relevant point defects. We will show that our first-principles calculations provide a valuable means for interpreting the experimental results. The calculations can aid in addressing the relevant point defects and diffusion mechanisms, and yield specific values for migration barriers. The computational techniques are those that have been previously applied to the investigation of ground-state configurations of point defects in GaN.[14,15] For consistency, we have repeated the ground-state calculations with a higher level of convergence. The present results are in good agreement with the earlier published values.[14,15] For our investigations of point-defect diffusion, we have focused on self-interstitials and vacancies. Antisites have high formation energies in GaN, and we have no reason to believe they play an important role under either equilibrium or nonequilibrium conditions. Since GaN has the wurtzite structure, one might expect an anisotropy in the diffusion of point defects. We have therefore systematically investigated migration paths parallel and perpendicular to the c axis. Our conclusion will be, however, that no anisotropy should be observed.

Section II describes our theoretical approach. Section III reports results for ground-state configurations and migration barriers for gallium and nitrogen interstitials, and gallium and nitrogen vacancies. A discussion of these results and comparison with experiment is contained in Sec. IV. Section V concludes and summarizes the paper.

II. THEORETICAL APPROACH

A. Total-energy calculations

Our first-principles calculations are based on density-functional theory[16] in the local-density approximation and *ab initio* norm-conserving pseudopotentials, with a plane-wave basis set.[17] We use the nonlinear core correction (*nlcc*),[18] with an energy cutoff of 40 Ry. It has been established that the *nlcc* provides an adequate description of the effects of the Ga $3d$, with the exception of the formation energy of the gallium vacancy, where the calculations with explicit inclusion of the $3d$ electrons yield a higher formation energy.[19]

All calculations were carried out at the theoretical lattice constant of bulk wurtzite GaN, which is $a^{theor}=3.09$ Å in the *nlcc* and $a^{theor}=3.18$ Å in the $3d$ calculations (compared with $a^{expt}=3.19$ Å). We used the ideal c/a ratio of $\sqrt{8/3}$ which is very close to the calculated c/a ratio of 1.633 (experiment: 1.627). We used 32-atom and 96-atom supercells. Details about supercell construction can be found in Ref. 20. We have used the 32-atom supercells to perform preliminary explorations of migration paths, and 96-atom supercells to investigate the ground-state and saddle-point configurations with higher accuracy. Unless otherwise mentioned, the results cited in this paper are for 96-atom supercells.

Brillouin-zone integrations were carried out with a regular spaced mesh of $n\times n\times n$ points in the reciprocal unit cell, shifted from the origin as in the Monkhorst-Pack method[21] and reduced by symmetry to a set of irreducible **k** points. We use $n=2$ which results in a set of three irreducible **k** points in the 32-atom cells (four **k** points in cases where the screw symmetry of the wurtzite structure is broken), and two **k** points in the 96-atom cells (or more when the symmetry is broken).

B. Formation energies

The energetics of migration paths and barriers depend on energy *differences* between different configurations of a defect. However, in order to interpret the results and relate them to experiment it is useful to also have information about the *formation energy*. The formation energy (E^f) is the energy needed to create a defect. The concentration of the defect is related to E^f by the expression

$$c=N_{\text{sites}}\exp(-E^f/kT), \tag{1}$$

where N_{sites} is the number of sites in the lattice (per unit volume) where the impurity can be incorporated, k is the Boltzmann's constant, and T is the temperature. This shows that the higher the formation energy the less likely the defect will form. The above relation, in principle, only holds in thermal-equilibrium conditions. However, the formation energy provides a useful measure of the likelihood of defect formation even under certain nonequilibrium conditions.

We illustrate the definition of the formation energy with the examples of a nitrogen vacancy (V_{N}) and a nitrogen interstitial (N_i):

$$E^f[V_{\text{N}}^q]=E_{tot}[V_{\text{N}}^q]-E_{tot}[\text{GaN,bulk}]+\mu_{\text{N}}+q[E_F+E_v], \tag{2}$$

$$E^f[\text{N}_i^q]=E_{tot}[\text{N}_i^q]-E_{tot}[\text{GaN,bulk}]-\mu_{\text{N}}+q[E_F+E_v]. \tag{3}$$

$E_{tot}[V_{\text{N}}^q]$ ($E_{tot}[\text{N}_i^q]$) is the total energy derived from a supercell calculation with one nitrogen vacancy (interstitial) in the cell, and $E_{tot}[\text{GaN,bulk}]$ is the total energy for the equivalent supercell containing only bulk GaN. q is the charge state of the defect, and μ_{N} is the chemical potential of N. E_F is the Fermi level, referenced to the valence-band maximum in the bulk. Due to the choice of this reference, we need to explicitly put in the energy of the bulk valence-band maximum, E_v. The position of E_v is adjusted to reflect the shift in average potential between the supercell containing the defect and the bulk. The chemical potential μ_{N} depends on the experimental growth condition which can be either N rich or Ga rich.[14,15] For purposes of plotting the formation energies, we choose Ga-rich conditions, corresponding to $\mu_{\text{Ga}}=\mu_{\text{Ga}}[\text{bulk}]$.

For charged defects, we added a jellium background to neutralize the supercell. We have not applied any additional corrections relating to the electrostatic interactions between charged defects induced by the periodic boundary conditions. Tests have shown that a simple correction based on the electrostatic energy of an array of point charges is inappropriate since it significantly overestimates the effect. The main focus of the present work is on migration barriers, which are energy differences between different configurations of the defect in the same charge state and therefore not sensitive to chargestate-dependent corrections.

All of the point defects introduce levels in the band gap of GaN; experimental detection of these levels often is an important means of identification of the defect. Calculation of these levels is therefore an important priority. The thermodynamic transition levels involve transitions between different charge states of the defect. This means that the Kohn-Sham levels that result from a band-structure calculation for the center in a single charge state cannot directly be identified with levels that are relevant for experiment. The thermodynamic transition level $\varepsilon(q_1/q_2)$ is defined as the Fermi-level position where charge states q_1 and q_2 have equal energy. As the name implies, this level would be observed in experiments where the final charge state can fully relax to its equilibrium configuration after the transition. This type of level is therefore what is observed, for instance, in deep-level transient spectroscopy experiments. Note that optical levels, as observed in photoluminescence, correspond to a situation where the final charge state does *not* relax to its equilibrium configuration after the transition. The levels observed in optical experiments may therefore differ from the thermodynamic transition levels.

III. RESULTS

A. Formation energies and transition levels

Formation energies for all the native point defects in GaN were previously reported in Refs. 14 and 15. Those results were obtained in 32-atom and 72-atom supercells. Our present study of point-defect diffusion employs 96-atom supercells; as part of this study we had to recalculate the

TABLE I. Formation energies of native defects in wurtzite GaN, calculated in 32-atom and 96-atom supercells (Ref. 25). The formation energies are shown for the Fermi level equal to the valence-band maximum, and Ga-rich conditions.

Defect	Charge state	E^f (eV) (Ga rich) 32-atom	96-atom
Ga_i	3+	2.47	2.34
	2+	5.09	4.89
	1+	7.88	7.28
N_i	3+	3.86	3.19
	2+	4.05	3.93
	1+	5.10	4.83
	0	6.86	6.31
	1−	9.12	8.31
	2−	13.33	12.90
	3−	17.18	17.34
V_N	3+	−0.89	−1.08
	1+	−0.01	0.10
V_{Ga}	0	8.10	9.06
	1−	8.29	9.31
	2−	9.08	9.95
	3−	10.46	11.05

ground-state configurations and formation energies. Values for formation energies are shown in Table I and Fig. 1. Only minor quantitative differences occur with respect to the previous work.[14,15] The corresponding thermodynamic transition levels for the defects discussed in this paper are illustrated in Fig. 2.

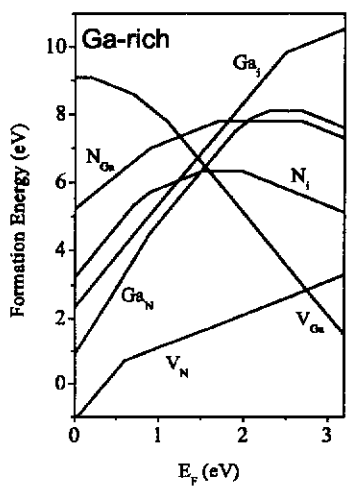

FIG. 1. Formation energies as a function of Fermi level for native point defects in GaN. Ga-rich conditions are assumed. The zero of Fermi level corresponds to the top of the valence band. Only segments corresponding to the lowest-energy charge states are shown. The slope of these segments indicates the charge state. Kinks in the curves indicate transitions between different charge states.

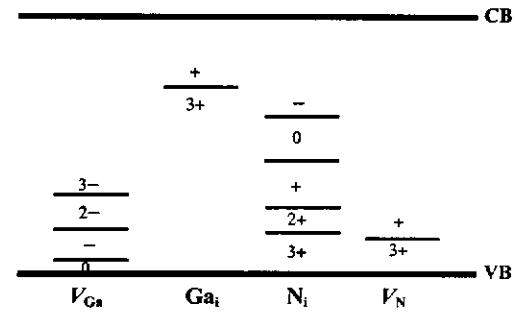

FIG. 2. Thermodynamic transition levels for defects in GaN, determined from formation energies listed in Table I and displayed in Fig. 1.

B. Gallium interstitial Ga_i

1. Atomic structure and energetics

The Ga interstitial can occur in the 3+, 2+, and 1+ charge states. We find that the neutral charge state is not stable, i.e., the $\varepsilon(+/0)$ transition level lies above the conduction-band minimum. Our calculations show that in wurtzite GaN, the gallium interstitial Ga_i^{3+} favors a site near the octahedral interstitial site, at the center of the hexagonal channel. We call this site O' to distinguish it from the ideal octahedral interstitial O site. At the O' site the distances to the six Ga nearest neighbors are roughly the same, to within 0.1 Å: they amount to 2.39 Å to one set of neighbors, and 2.47 Å to the other; this indicates that the interstitial atom positions itself so as to minimize repulsion from these Ga neighbors. In the process, the interstitial moves closer to the plane of its three nitrogen neighbors, at a Ga_i-N distance of 1.80 Å. This distance is shorter than for Ga-N bonds in the bulk crystal, indicating the presence of a favorable electrostatic interaction between the positively charged Ga_i^{3+} and the electronegative nitrogen host atoms.

The atomic structure is very similar in the other charge states: in the 2+ charge state the distances to the Ga neighbors are 2.39 Å and 2.44 Å, and the Ga_i-N distance is 1.86 Å. In the 1+ charge state, finally, the distances to all Ga neighbors are 2.40 Å, and the Ga_i-N distance is 1.90 Å. The increase in the distance to the nitrogen neighbors (which is accommodated mainly through the motion of the nitrogens) when the charge state is lowered from 3+ to 1+ indicates the importance of Coulomb attractions. Note that the mechanisms behind these configurations are very similar to those discussed for beryllium interstitials Be_i^{2+} in Ref. 20.

We also discovered an additional local minimum for Ga_i^{3+}, located between the T site and the O' site. This metastable minimum is similar to a configuration that we investigated for Be interstitials in GaN, and that we labeled the A site.[20] This local minimum has an energy only 0.38 eV higher than the global minimum. Similar to the O' site, the driving force for stability of this configuration seems to be the proximity of the interstitial to three N neighbors, with bond distances between 1.83 and 1.85 Å. Simultaneously, a Ga atom that would prevent the interstitial from approaching the nitrogen atoms moves away, undergoing a large displacement. This is the same Ga atom that will ultimately be kicked

out of its lattice site after completion of the migration step described below. We verified that this configuration was indeed a local minimum by starting the relaxation process from different initial configurations, and also by investigating displacements of the interstitial away from the minimum and checking that the configuration returned to the local minimum. We note that in the A configuration the Ga atom is located fairly close to three host Ga atoms, at distances of 2.27 Å and two times 2.51 Å; the next set of Ga atoms is at 2.85 Å.

As shown in Fig. 1, the stable charge states are 3+ and 1+, meaning that Ga_i always acts as a donor. Its formation energy is lowest (but still higher than that of the nitrogen vacancy) for Fermi-level positions near the valence-band maximum (VBM), i.e., under p-type conditions. The 2+ state is not thermodynamically stable, and the 1+ charge state is stable at Fermi levels above 2.5 eV, where the high formation energy renders its formation unlikely under equilibrium conditions. However, Ga interstitials can be induced by non-equilibrium processes, for instance in the irradiation experiments of Ref. 5.

2. *Diffusion*

The high formation energy of the Ga interstitial is caused by the large size of the Ga atom, which does not"fit" inside the interstitial space available in the GaN lattice with its small lattice parameters. One might therefore think that the Ga interstitial will also have trouble moving through this lattice, i.e., that the migration barrier will be high. This is not the case. In fact, the migration barrier is the *difference* in energy between the saddle-point and the ground-state configurations; if both are high in energy, their difference can be modest, resulting in a moderate barrier.

We have investigated migration paths parallel to the c axis ($||c$) as well as in directions perpendicular to the c axis ($\perp c$). In these investigations we were aided by our previous work on diffusion of beryllium interstitials in GaN.[20] First we tracked the migration path along the hexagonal channel, resulting in a barrier height of 3.0 eV. The variation of the potential energy along this path is very similar to that of Be_i^{2+} as shown in Fig. 8 of Ref. 20. Even the barrier height is the same, with a value of 3.0 eV. Further investigations showed, however, that another migration path exists with a much lower barrier.

In the case of the Be interstitial, migration along this path proceeds by the interstitial moving from its stable configuration at O' through a saddle point at the tetrahedral interstitial site (T) to an O' site within the same basal plane in an adjacent hexagonal channel. This whole process occurs with a much lower migration barrier (1.2 eV) than migration through the hexagonal channel (which cost about 3 eV for Be_i). A similar situation occurs for Ga_i, but now the diffusing atom is the same element as one of the host atoms, and therefore diffusion can proceed via the so-called interstitialcy mechanism. The whole process is illustrated step-by-step in Fig. 3.

Figure 4 shows a plot of the potential energy along the migration path. Modeling this migration path in a 96-atom cell was essential. Near the O' site the 32-atom-cell results

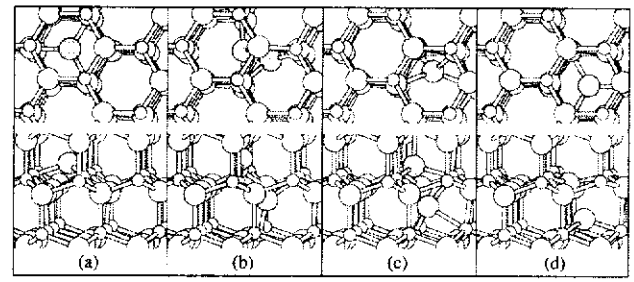

FIG. 3. Schematic illustration of the migration of a gallium interstitial via an interstitialcy mechanism. Top panels show a top view, lower panels a side view. (a) Ground state; (b) and (c) intermediate configurations along the migration path; (d) final configuration, after one migration step. Large circles represent Ga atoms, small circles N atoms, and shaded large circles highlight Ga atoms involved in the migration process.

are similar to the 96-atom-cell results, as can be seen from the formation energies in Table I. However, when the Ga_i atom starts to push the host Ga atom away from its lattice site, the relaxations extend over a volume that cannot be adequately modeled in a 32-atom cell.

The curve shown in Fig. 4 indicates the presence of a local minimum along the path, corresponding to the A site described in Sec. III B 1. At the A site the interstitial forms a split-interstitial configuration with a Ga host atom. When the interstitial is moved further towards T, it actually replaces the Ga host atom; i.e., it knocks the Ga host atom out of its lattice site, forcing it to become the new interstitial, which will move towards an O' site in an adjacent hexagonal channel.

This new O' site is located in a basal plane different from the site that was the starting point, implying that this migration path can apply to diffusion both parallel to c and per-

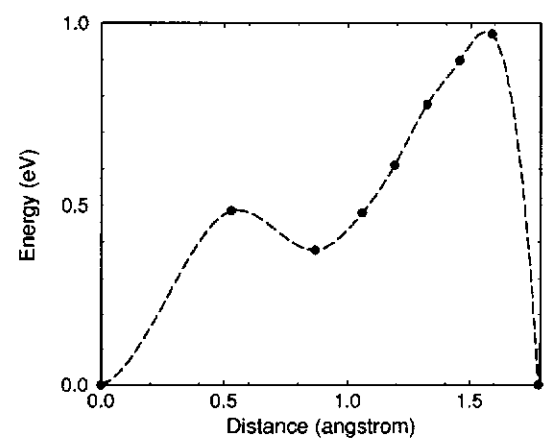

FIG. 4. Total energy (referenced to the ground-state configuration) of Ga_i^{3+} as a function of the horizontal distance of the Ga, atom measured from the center of the hexagonal channel towards the T site. All calculations were carried out in 96-atom supercells. The local minimum around ~0.9 Å corresponds to the A site. By the time the Ga_i has reached the T site, it has moved through a triangle of N atoms and replaced a Ga host atom, pushing the original Ga host atom off its lattice site to become the new Ga_i.

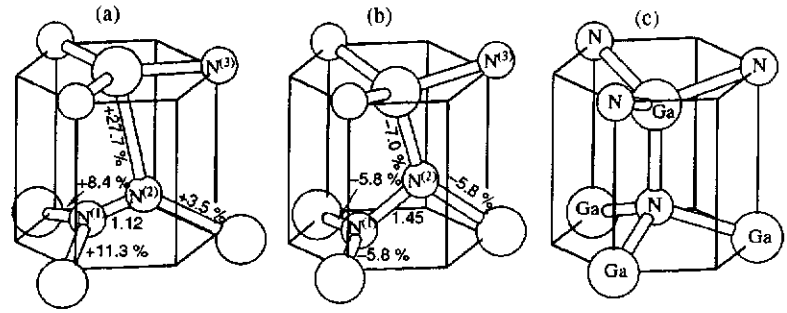

FIG. 5. Ball-and-stick model of atomic configurations of (a) N_i^{3+} and (b) N_i^- defects in GaN; (c) shows the equivalent section of bulk GaN for comparison. The N_i assumes a split-interstitial configuration. The hexagonal prisms are a guide to the eye, representing the symmetry of bulk GaN. Large spheres represent Ga atoms and small spheres N atoms. The percentages denote changes from the bulk Ga-N bond length. N-N bond lengths are expressed in angstroms. Note the outward relaxations of the surrounding Ga atoms: in the 3+ charge state, these Ga atoms move outwards over a distance equal to 25% of the Ga-N bond length; in the 1+ charge state, the corresponding number is 15%.

pendicular to c—unlike the case of the Be interstitial, where a clear anisotropy in the diffusion occurred. As shown in Fig. 4, the barrier along the migration path is about 0.9 eV.

Our most detailed investigations were carried out for the Ga interstitial in the 3+ charge state. However, our studies show a very similar migration path, with possibly slightly lower barriers, for the 2+ and 1+ charge states. The relative stability of the A site decreases when going from the 3+ to the 2+ to the 1+ charge state: in the 2+ charge state the A site is 0.6 eV higher in energy than O' (compared to 0.4 eV in the 3+ charge state), and in the 1+ charge state we did ıot succeed in stabilizing the A-site configuration.

C. Nitrogen interstitial N_i

1. Atomic structure and energetics

The ground state of the nitrogen interstitial consists of a split-interstitial configuration in which the N_i forms a N-N bond with one of the nitrogen host atoms, sharing its lattice site.[15] This configuration is energetically preferred, by a large margin, over other interstitial positions such as the octahedral (O) or tetrahedral (T) interstitial sites, due to the large strength of the N-N bond. The nitrogen interstitial can occur in various charge states, as shown in Fig. 1. The details of the atomic structure vary with the charge state of the defect, with the N-N bond distance varying from 1.45 in the 1− charge state to 1.12 in the 3+ charge, but the split-interstitial configuration is common to all charge states. Note that the N-N bond distances are comparable to the bond distance of N_2 (1.0975 Å). Since the host atom shares its lattice site with the interstitial, it is not clear which of the two atoms is the actual interstitial; both should be regarded on equal footing.

We show the atomic configurations for two of the charge states, N_i^{3+} and N_i^-, in Figs. 5(a) and 5(b). The common feature in all charge states is the bond formed between the N_i atom and a N host atom. We label the two N atoms as $N^{(1)}$ and $N^{(2)}$ for easy reference. There are four Ga atoms surrounding the site, and each N atom in the split interstitial forms bonds with two Ga atoms [see Fig. 5(a) and 5(b)].

For the 3+ charge state, the configuration could be viewed as a V_N^{3+} plus a N_2 dimer floating in the void. Indeed, the atomic positions as shown in Fig. 5(a) show large outward relaxations of the surrounding Ga atoms, with the Ga atoms being pushed into the plane of the surrounding N atoms; a similar relaxation is found in V_N^{3+}. In addition, the N-N bond distance of 1.12 Å is very close to the N_2 dimer bond distance. Clearly, in the 3+ charge state, the N-N pair is not eager to bond with the surrounding Ga atoms. As more electrons are added to the defect, the N-N bond becomes weaker (evidenced by the increased N-N distance) and the tendency to form bonds with the surrounding Ga atoms increases (evidenced by shorter Ga-N bond lengths). By the time four electrons are added (i.e., going from N_i^{3+} to N_i^-), the N-N bond distance is increased to 1.45 Å and both N atoms form strong bonds with their Ga neighbors, with an average bond distance that is 6.1 % *shorter* than the bulk Ga-N bond. The average bond distances for all charge states

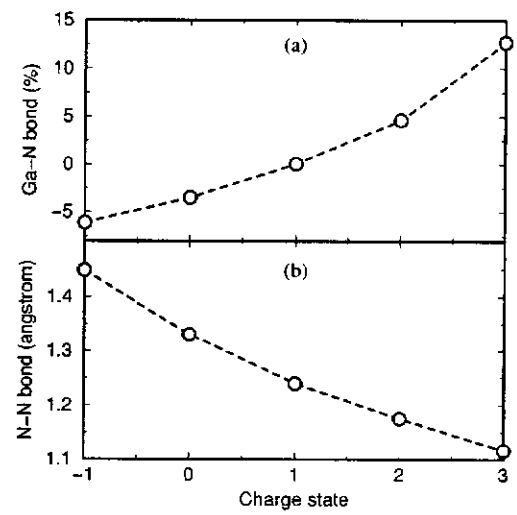

FIG. 6. Bond distances in the N_i split-interstitial defect as a function of charge state. (a) Percentage change (referenced to the bulk Ga-N bond length) of the average length between interstitial N atoms and the surrounding Ga atoms. (b) N-N bond distance in the split interstitial. Circles denote first-principles calculations, dashed lines serve as a guide to the eye.

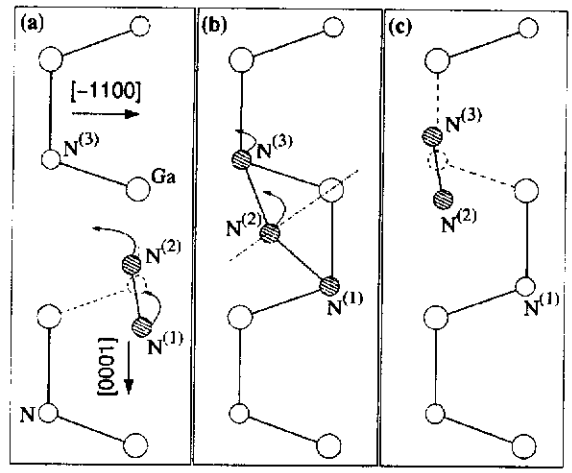

FIG. 7. Schematic illustration of the migration of a nitrogen interstitial via an interstitialcy mechanism. (a) Ground state. (b) Saddle-point configuration. (c) New ground state, after one migration step. Large circles represent Ga atoms, small circles N atoms, and shaded small circles highlight N atoms involved in the migration. Dashed circles indicate ideal atomic position of the lattice N, dashed lines bonds in the ideal lattice. The numbers in square brackets identify the migrating atoms.

are shown in Fig. 6(a). These results are in agreement with the results reported in Ref. 14, but more detail is provided here.

Nitrogen interstitials have fairly high formation energies for all Fermi-level positions (Fig. 1). They are thus unlikely to occur in thermal equilibrium. However, their formation may be induced under nonequilibrium conditions, for instance under irradiation. We find N^- to be the charge state with the highest number of electrons stable under *n*-type conditions. Wright[22] reported a $3-$ charge state, with a different atomic configuration, for Fermi levels above 3.17 eV. We do not find this charge state to be stable, and suggest that its occurrence in Ref. 22 is an artifact due to the occupancy of conduction-band states.

2. *Diffusion*

Nitrogen interstitials diffuse via an interstitialcy mechanism as illustrated in Fig. 7. Note that the atomic positions in Fig. 7 do not reflect the actual relaxations; the figure merely serves as a schematic for elucidating the diffusion process. Figure 7(a) illustrates N_i in the ground state (split-interstitial configuration); the interstitial ($N^{(1)}$) and one of the host atoms ($N^{(2)}$) share a lattice site and form a short (N_2-molecule-like) bond. At the start of the migration process, $N^{(2)}$ moves up, dragging $N^{(1)}$ along in an effort to keep the N-N bond short. Figure 7(b) illustrates the instant where $N^{(2)}$ is at the midpoint of the migration process, i.e., $N^{(2)}$ is located equidistant from $N^{(3)}$ and $N^{(1)}$. The actual positions of $N^{(1)}$ and $N^{(3)}$ at this saddle-point configuration depend strongly on the charge state. Finally, $N^{(2)}$ moves past the saddle point and continues to move to form a new split-interstitial configuration with $N^{(3)}$, leaving $N^{(1)}$, which was initially the interstitial, occupying a lattice site.

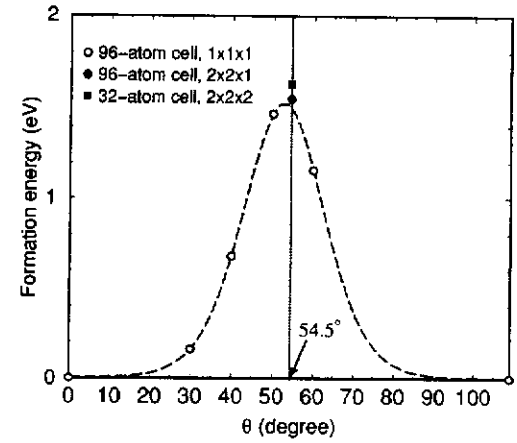

FIG. 8. Total energy (referenced to the ground state) of N_i^- along the migration path, as described in the text. Dashed lines are a guide to the eye.

The practical details of our calculations for the saddle-point configuration are as follows. We apply constraints to the atoms involved. First, we constrain $N^{(2)}$ in the plane bisecting the line connecting the two *ideal* lattice sites associated with $N^{(1)}$ and $N^{(3)}$. In Fig. 7(b), this plane is perpendicular to the plane of the figure; its projection is shown as a dot-dashed line. To ensure that $N^{(2)}$ is roughly equally far away from both $N^{(1)}$ and $N^{(3)}$, we also constrain the center of mass of $N^{(1)}$ and $N^{(3)}$ to be in this plane. All other atoms in the supercell are allowed to freely relax. The diffusion barriers obtained at the saddle points in 32-atom supercells are 1.6 eV for $1-$, 2.4 eV for 0, 2.1 eV for $1+$, 2.5 eV for $2+$, and 1.4 eV for $3+$ charge state.

For N_i^- we also performed calculations in a 96-atom supercell, both to verify the location of the saddle point and to test the convergence with respect to supercell size. Only one **k** point ($1\times1\times1$ sampling) was used in the Brillouin-zone integration for the calculations of the migration path, in order to reduce the computational demand. We subsequently checked the saddle-point configuration using a $2\times2\times1$ **k**-point set. In the calculations for the migration path, the diffusing atom [i.e., $N^{(2)}$ in Fig. 7(b)] was placed in various planes along the diffusion path. For this purpose, we generalized the plane constraining $N^{(2)}$ used in the calculations for the saddle-point configuration. Using the ideal position of the nearest Ga atom as a pivot point, we can define planes with different angle θ from the [0001] direction. With this convention, the plane used to calculate the saddle-point configuration has an angle $\theta = 109.5°/2 = 54.7°$. To check if the configuration assumed above indeed corresponds to the maximum in the energy along the path, we constrained the diffusing atom in various planes ($\theta = 30°, 40°, 50°, 60°$) and calculated the corresponding energies. The center of mass of $N^{(1)}$ and $N^{(3)}$ was not constrained in these calculations. The formation energy as a function of θ (see Fig. 8) shows the crest point near $\theta = 54.7°$, confirming that the configuration studied above indeed corresponds to the saddle point. Figure 8 also shows that the calculations at $\theta = 54.7°$ with different supercell sizes and **k**-point samplings give very similar mi-

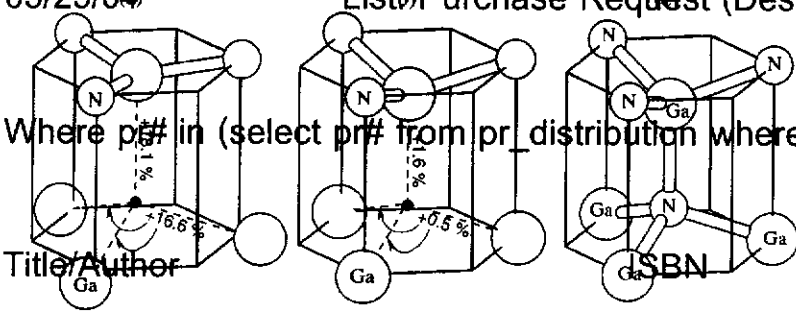

FIG. 9. Ball-and-stick model of atomic configurations of (a) V_N^{3+} and (b) V_N^{+} in wurtzite GaN. (c) shows the equivalent section of bulk GaN for comparison. Large spheres represent Ga atoms, small spheres N atoms, and the black circle the lattice site where the vacancy is created. The percentages denote the changes from the bulk Ga-N bond length.

gration barriers (to within 0.1 eV). These tests show that supercell size does not strongly affect the calculations for the migration barrier of N_i.

In addition to the diffusion process discussed above, N could also move in a direction perpendicular to [0001] ($\perp c$). This involves one of the N atoms in the split-interstitial configuration breaking away from its partner and traveling in the basal plane to bond with another N in the same plane. Using a 96-atom supercell, we obtained a barrier of 2.4 eV for N. This barrier is higher than the barrier of 1.6 eV for the process illustrated in Fig. 7. Since the process of Fig. 7 can result in motion both parallel to c and perpendicular to c, diffusion along both directions will be governed by the same barrier; i.e., no anisotropy will occur.

D. Nitrogen vacancy V_N

1. Atomic structure and energetics

Figure 1 shows that the stable charge states for V_N are 1+ and 3+ in agreement with Ref. 15. Calculations for the ground state of both charge states were performed in 96-atom supercells. This is particularly important for the 3+ charge state, which exhibits large lattice relaxations. The relaxed atomic structures from the 96-atom-cell calculations are shown in Fig. 9. Note the large outward relaxations of the Ga atoms surrounding the vacancy in the 3+ charge state. This large breathing relaxation has been found also in other semiconductors such as GaAs (Ref. 23) and ZnSe.[24] In the 1+ charge state, the breathing relaxation is quite small, amounting to 1.6% of the experimental bond length for the Ga neighbor along the c axis, and 0.5% for the other three Ga neighbors (or 0.8% on average). The breathing relaxation is much larger in the 3+ charge state, where the Ga neighbors move outward by 18.1% ($||c$) and 16.6%, or 17.0% on average.

Nitrogen vacancies have low enough energies to occur under thermal-equilibrium conditions in p-type GaN. The stable charge states for V_N in GaN are 1+ and 3+. The 2+ charge state is never stable; this is characteristic of a negative-U impurity, and is usually associated with a strikingly large lattice relaxation of one of the charge states; here this is the case for the 3+ charge state. The ionization level $\varepsilon(3+/1+)$ between the 3+ and 1+ charge states occurs at $E_F = E_V + 0.18$ eV, somewhat higher than the value of 0.16 eV value reported in Ref. 15 due to the larger supercell size used here. This means the 3+ charge state is stable under p-type conditions, and its low formation energy indicates that nitrogen vacancies can be a serious source of compensation in p-type GaN. Note that the formation energy of V_N^+ increases with the Fermi level (see Fig. 1), so that nitrogen vacancies are unlikely to occur in n-type GaN.[14]

2. Diffusion

We obtained the migration barrier of the nitrogen vacancy by calculating the energy needed to move a nitrogen atom from its nominal lattice adjacent to the vacancy along a path towards the vacancy, leaving a vacancy behind at the original lattice site. The path is illustrated in Fig. 10. We define the coordinate along the path as the angle θ of the bond between the migrating N atom and the ideal lattice site of the Ga atom at the pivot point, measured from the [0001] direction. The energy as a function of angle θ for V_N^{3+} is shown in Fig. 11. The 32-atom-cell results provide an estimate of the migration barrier for charge state 3+ of 2.0 eV at $\theta \approx 40°$. Calculations in a 96-atom cell for $\theta = 40°$ and 50° provide a more accurate migration barrier for V_N^{3+} of 2.6 eV. The difference is mainly due to the higher ground-state energy in the 32-atom cell, which is too small to properly accommodate the large relaxations in the 3+ charge state.

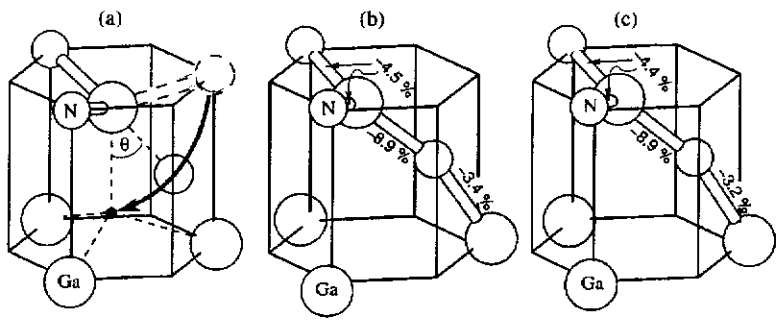

FIG. 10. Ball-and-stick model of atomic positions describing the diffusion process of V_N. (a) Schematic illustration of the migration path. (b) Saddle-point configuration for V_N^{3+}. (c) Saddle-point configuration for V_N^{+}. Large spheres represent Ga atoms, small spheres N atoms, and the black dots the ideal lattice site of the vacancy. The percentages denote the changes from the bulk Ga-N bond length.

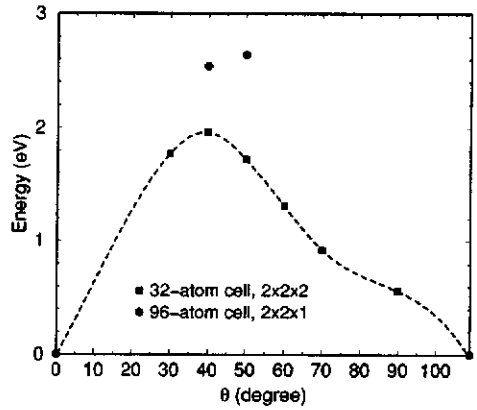

FIG. 11. Total energy (referenced to the ground state) of V_N^{3+} during the diffusion process.

Surprisingly, for the nitrogen vacancy in the 1+ charge state (V_N^+) we obtain a much higher migration barrier of 4.3 eV . We propose the following explanation for this large difference in migration barriers between different charge states: for V_N^+, the saddle-point configuration can be regarded as a complex consisting of two nitrogen vacancies and one nitrogen interstitial: $2V_N^+ + N_i^-$, where the charges have been chosen such that the total charge of the complex (1+) is maintained. Similar arguments for the saddle point of V_N^{3+} suggest a complex consisting of $2V_N^+ + N_i^+$. The energy of the $2V_N + N_i$ complex will differ mainly due to the different charge on N_i (assuming no change in binding energy of the complex). If we now assume that the Fermi level is 0.5 eV above the VBM (a typical value if we want V_N^{3+} to be stable) then the energy difference between $2V_N^+ + N_i^-$ and $2V_N^+ + N_i^+$ is 2.5 eV. This difference is consistent with the large difference in migration barriers between V_N^+ and V_N^{3+}.

The migration path described above can account for motion along the c axis ($||c$) as well as in directions perpendicular to the c axis ($\perp c$). We have also studied a migration path that would account exclusively for in-plane ($\perp c$) diffusion, by moving a nitrogen atom from the same basal plane as the vacancy towards the vacancy. Note that this path would be relevant only if it results in a lower barrier than the barriers calculated above, since diffusion $\perp c$ can also be accomplished via the diffusion process described above. Our calculated migration barriers for the in-plane motion were higher than the ones calculated above for both charge states. Therefore, migration of V_N^+ and V_N^{3+} will be governed by the same barriers for diffusion $||c$ and $\perp c$. No anisotropy should be observed.

E. Gallium vacancy V_{Ga}

1. Atomic structure and energetics

Figure 1 shows that gallium vacancies have lowest energies in the 3− charge state, which occurs in n-type material.[25] Under those circumstances V_{Ga} may act as a compensating center (a triple acceptor). The nitrogen atoms around a gallium vacancy exhibit an outward breathing relaxation: in the 3− charge state the N atoms move outward by ≈4% (referenced to the experimental bond length).

The Ga vacancy has a deep level (the 2−/3− transition level) about 1.1 eV above the valence band. Transitions between the conduction band (or shallow donors) and this deep level would therefore result in emission around 2.3 eV. The gallium vacancy has therefore been proposed as the source of the "yellow luminescence."[26]

2. Diffusion

Our investigations of gallium vacancies were performed using an approach similar to that described in Sec. III D 2 for nitrogen vacancies: a neighboring Ga atom was moved towards the vacancy and the potential energy along that path was evaluated. A migration barrier of 1.9 eV was obtained (in a 96-atom cell) for V_{Ga}^{3-}, the most relevant charge state.

IV. DISCUSSION AND COMPARISON WITH EXPERIMENT

Our calculations produce values for migration barriers. In order to derive diffusion coefficients D, we would also need to know the prefactor D_0 in the expression $D = D_0 \exp(-E_b/kT)$. Accurate calculations of the prefactor are beyond the scope of the present investigation, but a rough estimate can be obtained using the expression $D_0' = \alpha \nu a^2 \exp(\Delta S/k)$, where α is a geometry-related factor, ν is an attempt frequency, a is the spacing between sites, and ΔS is the diffusion entropy. $\alpha \nu a^2$ is typically in the range of 0.001–1 m^2/s; a larger value of D_0' is indicative of a large entropy contribution.

Comparisons with experiment often rely on identifying the temperature at which a particular defect becomes mobile. A reasonable estimate of this temperature can be obtained by taking the usual definition of an activation temperature, i.e., the temperature at which the jump rate is 1 per second, and assuming a prefactor of 10^{13} s^{-1}, i.e., a typical phonon frequency.

A. Gallium interstitial Ga_i

Obtaining accurate results for the atomic configuration of the gallium interstitial is difficult due to the fairly large lattice relaxations induced by this defect. The calculations reported in Refs. 14 and 15 found the octahedral site to be most stable for Ga_i. In contrast, in Ref. 27 it was argued that the tetrahedral site was slightly more stable than the O site. Based on our recent 96-atom supercells we can now confidently state that the octahedral interstitial site, at the center of the hexagonal channel, is the stable site for Ga_i in all charge states. The T site is not a local minimum, but plays a role in the diffusion process.

Detailed experimental data are available for the gallium interstitial. Using EPR, Chow *et al.*[5] studied point defects created by electron irradiation at low temperature (4.2 K). They were able to unambiguously identify the Ga interstitial, and their annealing studies indicated that this interstitial becomes mobile at temperatures slightly below room temperature. An activation energy of 0.7 eV was estimated. Our calculations showed that migration of the Ga interstitial can

proceed with a barrier of 0.9 eV or less, in good agreement with the experimental observations of Ref. 5.

In the experiments of Ref. 5, *n*-type material was used, and therefore the thermodynamically stable charge state was likely to be 1+. The EPR technique requires an unpaired electron to be present in the level, which in the case of Ga_i occurs for the 2+ charge state. Note that we found this charge state to be thermodynamically unstable, due to the negative-*U* character. However, the experiments of Ref. 5 are based on optical detection of EPR (ODEPR), in which the sample is excited with ultraviolet light. This excitation can lead to formation of the 2+ charge state, which in thermal equilibrium would not be stable.

B. Nitrogen interstitial N_i

Our calculated migration barriers indicate that nitrogen interstitials could become mobile at temperatures around 200 °C, at least for the 1− and the 3+ charge states (which are probably most likely to occur, under *n*-type, and *p*-type conditions respectively). We are not aware of any experiments in which the diffusion of nitrogen interstitials has been directly observed.

C. Nitrogen vacancy V_N

Hautakangas *et al.*[9] recently carried out positron-annihilation studies of Mg-doped GaN grown by metal-organic chemical vapor deposition (MOCVD). They detected the presence of V_N-Mg_{Ga} pairs, at a concentration of 10^{17}–10^{18} cm^{-3}. The concentration of nitrogen vacancies decreased upon annealing at 500–800 °C; an activation energy of 3.0 eV was estimated for the process of vacancy removal. This activation energy would be the sum of the migration barrier for the vacancy and the binding energy of the V_N-Mg_{Ga} pair. The latter has been calculated[28] to be 0.5 eV, resulting in an estimate for the migration barrier of 2.5 eV. This value is very close to our calculated barrier of 2.6 eV for V_N^{3+}.

Diffusion experiments of a different kind were carried out by Ambacher *et al.*,[1] who measured self-diffusion in $Ga^{14}N/Ga^{15}N$ isotope structures grown by molecular-beam epitaxy (MBE). Diffusion profiles before and after thermal annealing at temperatures of 800 °C and 900 °C were measured by secondary-ion mass spectroscopy (SIMS). The activation enthalpy for diffusion was found to be 4.1 ±0.4 eV. The samples were *n* type, with the Fermi level close (within 30 meV) to the conduction band. This value agrees well with our calculated migration barrier for V_N^+. We note that, in general, the activation enthalpy corresponds to the sum of the formation energy and migration energy of the defect responsible for diffusion. The fact that the activation enthalpy of Ref. 1 corresponds to just the migration barrier can be attributed to the presence of a nonequilibrium concentration of vacancies in the samples, eliminating the cost of forming the defects responsible for self-diffusion. Arguments to support this will be presented elsewhere.[29] This point of view is consistent with thermal decomposition experiments presented by Ambacher in the same paper,[1] in which an activation energy of 3.9±0.2 eV was found, again consistent with migration of V_N^+. In this case, the surface acts as a source of vacancies, again eliminating the cost of defect formation from the activation energy.

Even though our calculated migration barrier for V_N^+ is high (4.3 eV), it still allows the nitrogen vacancy to be mobile at typical MOCVD growth temperatures, particularly when the large entropy reported by Ambacher *et al.*[1] is taken into account. In MBE, however, where the growth temperatures are much lower, nitrogen vacancies are not mobile during growth. Consequences will be discussed in Ref. 29.

D. Gallium vacancy V_{Ga}

Gallium vacancies (V_{Ga}^{3-}) have relatively low formation energies in highly doped *n*-type material (E_F high in the gap); they could therefore act as compensating centers. Yi and Wessels[30] have found evidence of compensation by a triply charged defect in Se-doped GaN. Our results for gallium vacancies are in good agreement with the positron-annihilation experiments of the group of Saarinen. In Ref. 7 they showed that concentrations of gallium vacancies are higher in *n*-type material than in *p*-type or semi-insulating material, consistent with our calculated formation energies (Fig. 1). They also showed that gallium vacancies have higher concentrations in oxygen-rich material, consistent with the prediction[26,31] that a V_{Ga}-O complex can form with a binding energy of 1.8 eV.

Our theoretical results indicate that the gallium vacancy could give rise to a variety of transitions in the yellow and green regions of the spectrum. The transition level between the 3− and 2− charge states of the isolated vacancy occurs at 1.1 eV above the VBM (Ref. 26 and Fig. 2), which formed the basis for the prediction that gallium vacancies are responsible for the frequently observed yellow luminescence, a broad luminescence band centered around 2.2 eV. However, the 2−/1− transition level occurs at only slightly lower energy (which would push the emission towards the green). Complex formation with oxygen also pushes the level down (i.e., towards green emission). These results may well explain the observations of green and yellow luminescence in freestanding GaN templates by Reshchikov *et al.*[32]

Saarinen *et al.*[8] also applied positron-annihilation spectroscopy to study thermal annealing of gallium vacancies. Vacancies induced by electron irradiation were found to anneal out in long-range migration processes at 500–600 K with an estimated migration energy of 1.5 eV, in reasonable agreement with our calculated migration barrier of 1.9 eV. Native Ga vacancies in as-grown GaN, on the other hand, survived up to much higher temperatures (1300–1500 K), leading to the conclusion that they are stabilized by forming complexes with oxygen impurities. The estimated binding energy of 2.2 eV of such complexes is in agreement with the theoretical predictions.[26,31]

Bozdog *et al.*[3] reported that the *L*1 signal observed by ODEPR in electron-irradiated material is stable up to ~500 °C; Watkins *et al.* also proposed that *L*1 is associated with V_{Ga}.[4] Our calculated migration barrier of 1.9 eV for V_{Ga} is in qualitative agreement with this annealing behavior.

TABLE II. Migration barriers for native defects in wurtzite GaN. As discussed in the text, the lowest-energy migration paths result in atomic motion both parallel (||) and perpendicular (⊥) to the c axis; the diffusion is therefore isotropic in all cases. All values are from 96-atom supercell *nlcc* calculations, except for N_i in the 3+, 2+, 1+, and 0 charge states, where 32-atom supercells were used.

Defect	Charge state	Barrier (eV)
Ga_i	3+	0.9
	2+	≤0.9
	1+	≤0.9
N_i	3+	1.4
	2+	2.5
	1+	2.1
	0	2.4
	1−	1.6
V_N	3+	2.6
	1+	4.3
V_{Ga}	3−	1.9

We can also comment on self-diffusion of the gallium species in GaN. In p-type material, this is most likely to occur via gallium interstitials, since the formation energy of the gallium vacancy is very high (see Fig. 1). In n-type material, on the other hand, gallium interstitials are unfavorable and diffusion is likely to proceed mediated by gallium vacancies. The activation energy for self-diffusion is the sum of the formation energy of the defect and the migration energy. Under n-type conditions, the formation energy of V_{Ga}^{3-} is in the range of 1–2 eV. Adding the migration energy, the activation energy for self-diffusion would be between 3 and 4 eV. An activation energy of 3 eV would imply that self-diffusion due to gallium vacancies could occur at temperatures around 800 °C. This is certainly consistent with the notion that gallium vacancies play a role in interdiffusion of InGaN quantum wells, as discussed in Ref. 10. Chuo *et al.*[12] also reported an activation energy of 3.4±0.5 eV for interdiffusion of In and Ga in InGaN/GaN quantum wells, which they attributed to vacancy-controlled second-nearest-neighbor hopping.

E. Impurity diffusion

Finally, we discuss two experimental results on impurity diffusion. Munkholm *et al.* obtained an approximate diffusion coefficient for Si in GaN of 3.5×10^{-18} cm^2/s at 810 °C. Assuming a typical prefactor in the range of 0.001–1 cm^2/s, the corresponding activation energy would be in the range of 3.1–3.8 eV. As discussed in Sec. IV D, this is consistent with the expected activation energy for a diffusion process that would be assisted by gallium vacancies.

Xing *et al.*[13] examined Mg redistribution in GaN epilayers grown by a combination of MOCVD and MBE. Their analysis of the SIMS profiles yielded a diffusion coefficient of 3×10^{-15} cm^2/s at 1160 °C. Assuming a typical prefactor in the range of 0.001–1 cm^2/s, the corresponding activation energy would be in the range of 3.3–4.2 eV. This could be consistent with a process involving gallium vacancies, as pointed out above in the case of Si diffusion. However, a distinction needs to be made between n- and p-type layers. Some of the experiments of Ref. 13 involved Mg diffusing into Si-doped layers, in which gallium vacancies can easily form, and the measured activation energy would be consistent with a diffusion process assisted by gallium vacancies. Within the p-type layer itself, however, gallium vacancies have high formation energies and therefore Ga-site impurities are more likely to diffuse by a mechanism involving interstitials. The formation energy of the Ga_i^{3+} interstitial under p-type conditions can be as low as 2.3 eV, and our calculated migration barrier is 0.9 eV, yielding an activation energy around 3.2 eV. The actual migrating species in that case would be a Mg interstitial, of course, for which the formation energy under p-type conditions was found to be about 2 eV.[33] We have not performed calculations for migration of the Mg interstitial. However, qualitatively a mechanism involving interstitials seems consistent with the observed Mg diffusion in p-type GaN.

V. CONCLUSIONS

We have presented detailed calculations for formation energies and migration paths for relevant native point defects in GaN. The main results are summarized in Tables I and II. In all cases the lowest-energy migration path moves the defect both parallel and perpendicular to the c axis; no anisotropy should therefore be observed in point-defect migration. Diffusion on the gallium sublattice is most likely to be mediated by gallium interstitials in p-type material, with a migration barrier ≤0.9 eV, while gallium vacancies are more favorable under n-type conditions, with a migration barrier of 1.9 eV. For the nitrogen sublattice, the nitrogen vacancy is more likely to form under p-type conditions and also has a lower migration barrier then. Both the formation energy and migration energy of the nitrogen vacancy are high under n-type conditions. Nitrogen interstitials have modest migration barriers, but their formation energies are high. We have discussed several cases in which our results can be directly correlated with experiment. However, systematic experimental studies of point-defect diffusion in nitride semiconductors would be highly valuable.

ACKNOWLEDGMENTS

We acknowledge useful discussions with E. E. Haller, J. Neugebauer, J. Northrup, and G. Watkins. This work was supported in part by the Air Force Office of Scientific Research, Contract No. F4920-00-C-0019, monitored by G. Witt, and by the Defense Advanced Research Projects Agency SUVOS program under SPAWAR Systems Center Contract No. N66001-02-C-8017, monitored by Dr. J. Carrano. The work in Thailand was supported by the Thai Research Fund, Contract No. BRG4680003.

[1] O. Ambacher, F. Freudenberg, R. Dimitrov, H. Angerer, and M. Stutzmann, Jpn. J. Appl. Phys., Part 1 **37**, 2416 (1998).
[2] M. Linde, S.J. Uftring, G.D. Watkins, V. Härle, and F. Scholz, Phys. Rev. B **55**, 10 177 (1997).
[3] C. Bozdog, H. Przybylinska, G.D. Watkins, V. Härle, F. Scholz, M. Mayer, M. Kamp, R.J. Molnar, A.E. Wickenden, D.D. Koleske, and R.L. Henry, Phys. Rev. B **59**, 12 479 (1999).
[4] G.D. Watkins, L.S. Vlasenko, and C. Bozdog, Physica B **308–310**, 62 (2001).
[5] K.H. Chow, G.D. Watkins, A. Usui, and M. Mizuta, Phys. Rev. Lett. **85**, 2761 (2000).
[6] M. Lannoo and J. Bourgoin, *Point Defects in Semiconductors I* (Springer-Verlag, Berlin, 1981), p. 219.
[7] J. Oila, V. Ranki, J. Kivioja, K. Saarinen, P. Hautojärvi, J. Likonen, J.M. Baranowski, K. Pakula, T. Suski, M. Leszczynski, and I. Grzegory, Phys. Rev. B **63**, 045205 (2001).
[8] K. Saarinen, T. Suski, I. Grzegory, and D.C. Look, Phys. Rev. B **64**, 233201 (2001).
[9] S. Hautakangas, J. Oila, M. Alatalo, K. Saarinen, L. Liszkay, D. Seghier, and H.P. Gislason, Phys. Rev. Lett. **90**, 137402 (2003).
[10] L.T. Romano, M.D. McCluskey, C.G. Van de Walle, J.E. Northrup, D.P. Bour, M. Kneissl, T. Suski, and J. Jun, Appl. Phys. Lett. **75**, 3950 (1999).
[11] A. Munkholm, G.B. Stephenson, J.A. Eastman, O. Auciello, M.V. Ramana Murty, C. Thompson, P. Fini, J.S. Speck, and S.P. DenBaars, J. Cryst. Growth **221**, 98 (2000).
[12] C.-C. Chuo, C.-M. Lee, and J.I. Chyi, Appl. Phys. Lett. **78**, 314 (2001).
[13] H. Xing, D.S. Green, H. Yu, T. Mates, P. Kozodoy, S. Keller, S.P. DenBaars, and U.K. Mishra, Jpn. J. Appl. Phys., Part 1 **42**, 50 (2003).
[14] J. Neugebauer and C.G. Van de Walle, Phys. Rev. B **50**, 8067 (1994).
[15] J. Neugebauer and C. G. Van de Walle, Festkörperprobleme/ Advances in Solid State Physics, Vol. 35, edited by R. Helbig (Vieweg, Braunschweig, 1996), p. 25.
[16] P. Hohenberg and W. Kohn, Phys. Rev. **136**, B864 (1964); W. Kohn and L.J. Sham, Phys. Rev. **140**, A1133 (1965).
[17] M. Bockstedte, A. Kley, J. Neugebauer, and M. Scheffler, Comput. Phys. Commun. **107**, 187 (1997).
[18] S.G. Louie, S. Froyen, and M.L. Cohen, Phys. Rev. B **26**, 1738 (1982).
[19] J. Neugebauer and C.G. Van de Walle, in *Diamond, SiC and Nitride Wide Bandgap Semiconductors*, edited by C. H. Carter, Jr., G. Gildenblat, S. Nakamura, and R. J. Nemanich, Mater. Res. Soc. Symp. Proc. No. 339 (Materials Research Society, Pittsburgh, 1994), p. 687.
[20] C.G. Van de Walle, S. Limpijumnong, and J. Neugebauer, Phys. Rev. B **63**, 245205 (2001).
[21] H.J. Monkhorst and J.D. Pack, Phys. Rev. B **13**, 5188 (1976).
[22] A.F. Wright, J. Appl. Phys. **90**, 6526 (2001).
[23] J.E. Northrup and S.B. Zhang, Phys. Rev. B **50**, 4962 (1994).
[24] A. Garcia and J.E. Northrup, Phys. Rev. Lett. **74**, 1131 (1995).
[25] For the gallium vacancy the ground-state formation energies have been calculated with inclusion of the $3d$ electrons as valence states (Ref. 19). Such calculations are prohibitively expensive in a 96-atom supercell. The 96-atom results were therefore obtained based on the 32-atom results including the $3d$ states, and a correction term derived from the difference between the 32-atom and 96-atom results using the *nlcc*.
[26] J. Neugebauer and C.G. Van de Walle, Appl. Phys. Lett. **69**, 503 (1996).
[27] P. Boguslawski, E.L. Briggs, and J. Bernholc, Phys. Rev. B **51**, 17 255 (1995).
[28] C.G. Van de Walle, J. Neugebauer, C. Stampfl, M.D. McCluskey, and N.M. Johnson, Acta Phys. Pol. A **96**, 613 (1999).
[29] C. G. Van de Walle, J. Neugebauer, and S. Limpijumnong (unpublished).
[30] G.-C. Yi and B.W. Wessels, Appl. Phys. Lett. **69**, 3028 (1996).
[31] T. Mattila and R.M. Nieminen, Phys. Rev. B **55**, 9571 (1997).
[32] M.A. Reshchikov, H. Morko, S.S. Park, and K.Y. Lee, Appl. Phys. Lett. **78**, 3041 (2001).
[33] J. Neugebauer and C.G. Van de Walle, in *Gallium Nitride and Related Materials*, edited by R. D. Dupuis, J. A. Edmond, F. A. Ponce, and S. Nakamura, Mater. Res. Soc. Symp. Proc. No. 395 (Pittsburgh, 1996), p. 645.